

Toward Unobtrusive Patient Handling Activity Recognition for Injury Reduction Among At-Risk Caregivers

Feng Lin, *Member, IEEE*, Aosen Wang, *Student Member, IEEE*, Lora Cavuoto, and Wenya Xu, *Member, IEEE*

Abstract—Nurses regularly perform patient handling activities. These activities with awkward postures expose healthcare providers to a high risk of overexertion injury. The recognition of patient handling activities is the first step to reduce injury risk for caregivers. The current practice on workplace activity recognition is based on human observational approach, which is neither accurate nor projectable to a large population. In this paper, we aim at addressing these challenges. Our solution comprises a smart wearable device and a novel spatio-temporal warping (STW) pattern recognition framework. The wearable device, named Smart Insole 2.0, is equipped with a rich set of sensors and can provide an unobtrusive way to automatically capture the information of patient handling activities. The STW pattern recognition framework fully exploits the spatial and temporal characteristics of plantar pressure by calculating a novel warped spatio-temporal distance, to quantify the similarity for the purpose of activity recognition. To validate the effectiveness of our framework, we perform a pilot study with eight subjects, including eight common activities in a nursing room. The experimental results show the overall classification accuracy achieves 91.7%. Meanwhile, the qualitative profile and load level can also be classified with accuracies of 98.3% and 92.5%, respectively.

Index Terms—Patient handling activity (PHA), plantar pressure, smart insole, spatio-temporal warping (STW), wearable health.

I. INTRODUCTION

OVERALL 19 million people, nearly 14% of the U.S. workforce, are employed in healthcare industries [1]. Overexertion injuries are the leading source of workers compensation claims and costs in healthcare settings. According to the data from Bureau of Labor Statistics, U.S. Department of Labor, workforces in hospitals and nursing homes, especially nursing aids, are at the highest risk of sustaining an overexertion injury [2]. Nurses and nursing assistants are among the top five

occupations with the highest injury rates and U.S. hospitals report 6.8 work-related injuries per 100 full-time employees, higher than construction and manufacturing workers [3]. These rates likely under-represent the true injury incidence as 24% of nurses and nursing assistants have reported using sick leave to recover from their work [4] and eight of ten nurses report frequent pain during work [5]. In 2012 alone, overexertion injuries, such as musculoskeletal disorders, low back pain and shoulder pain, account for nearly 70 million physician office visits in the U.S. annually, and an estimated 130 million total health care encounters including outpatient, hospital, and emergency room visits [6]. The related economic burden estimates, including compensation costs, lost wages, and lost productivity, are about 128 billion U.S. dollars [6]. As a consequence, work-related injuries represent a significant economic burden, involve substantial adverse personal outcomes, and can result in significant turnover of the nursing workforce [7], [8]. Preventing a nursing shortage, meeting patient care needs, improving nurse job satisfaction, and determining regulatory compliance are dependent on addressing the patient and material handling activities leading to pain and injury.

One of the reasons for the high injury rate with caregivers is the lack of a sophisticated approach to timely detection of injury development and proactive prevention, e.g., physical therapy [9] or workload rescheduling [10]. How to best quantify workplace conditions, particularly physical exposures experienced by the worker, remains an open research question [11]. Currently, the best practice of exposure assessment often relies on visual inspection performed by an observer. Because of limitations of an individual observer, sampling methods are applied such that only a few workers are typically observed and only for a relatively short duration [12], [13]. In addition, observation-based approaches are often subjective, failing to integrate multifaceted traits or provide accurate quantification of physical exposures [14]–[16].

Recent advances in technology allow for the possibility of more dynamic assessment and monitoring of patients and older individuals across a variety of key medical scenarios: remote rehabilitation coaching, long-term care, home, and assisted living. Similar views have been also echoed by occupational safety investigators. Existing work can be summarized into two categories, i.e., ambient sensing systems and wearable sensing systems. The ambient sensing systems are integrated into the

Manuscript received November 8, 2015; revised March 1, 2016; accepted April 4, 2016. Date of publication April 6, 2016; date of current version May 3, 2017.

F. Lin, A. Wang, and W. Xu are with the Department of Computer Science and Engineering, University at Buffalo, the State University of New York (SUNY), Buffalo, NY 14260, USA (e-mail: flin28@buffalo.edu; aosenwan@buffalo.edu; wenyaxu@buffalo.edu).

L. Cavuoto is with the Department of Industrial and Systems Engineering, University at Buffalo, the State University of New York, Buffalo, NY 14260, USA (e-mail: loracavu@buffalo.edu).

Digital Object Identifier 10.1109/JBHI.2016.2551459

environment and less obtrusive to users. The most successful example of ambient sensing system is the computer vision system (including normal video, thermal, infrared, and depth cameras) for monitoring the work conditions, user motion, and behavior in nursing rooms [17], [18]. These methods involve costly installation and maintenance effort [18]. Moreover, there are still several technical challenges regarding immobility, occlusion, varying illuminations, and privacy invasion [19], [20]. Wearable sensing systems, such as a miniaturized inertial motion unit (IMU), are suggested to monitor occupational health and safety [11], [21], [22]. Most of the current workplace sensor applications have focused on posture analysis [22], task classification [11], basic physiological monitoring [23], [24], or a computerized application of traditional observational tools [25]. Although the applications of these systems have been primarily in general manual materials handling, manufacturing, or construction tasks, wearable sensor is still a promising approach to caregiver monitoring due to the similar nature of the tasks performed. However, to monitor complex patient handling activities, multiple IMU sensors on different body locations are often needed [26], [27], which is not convenient for long-term use and may even disrupt the normal work flow in the nursing room [28], [29].

Compared with daily life activity recognition [30], patient handling activity (PHA) recognition is a challenging and substantially unexplored topic. PHA is a complex process and usually involves an interactive procedure between healthcare workers and loads (e.g., patients, medical instruments). The characterization of PHA includes not only body postures but loads. For example, transferring a 60-pound patient from wheelchair to bed is significantly different from that activity with a 300-pound patient.

In this study, we propose a solution to overcome the aforementioned obstacles in PHA recognition, which comprises a Smart Insole 2.0 and a spatio-temporal warping (STW) pattern recognition framework. Smart Insole 2.0 utilizes an advanced electronic textile (eTextile) fabric sensor technique providing accurate plantar pressure measurement in both ambulatory and static status. Furthermore, Smart Insole 2.0 is unobtrusive, just like a normal insole without any extra cable, antenna, or adhesive equipment. The STW pattern recognition framework is proposed to quantify the similarity among different PHAs by exploiting the plantar pressure attributes in spatial and temporal domains with a novel warped spatio-temporal distance (WSTD). We perform a pilot study with eight subjects including eight common activities in nursing room. The experimental results show our method succeeds in qualitative profile recognition, PHA recognition, and load estimation with the overall classification accuracy of 98.3%, 91.7%, and 92.5%, respectively.

The organization of the remaining paper is as follows. Section II introduces the related work and sensing modalities. Section III provides the overall system diagram and the feasibility of using plantar pressure for PHA recognition. In Section IV, we describe the hardware and software design on smartphone for Smart Insole 2.0. Section V elaborates the WSTD algorithm. Section VI describes the STW pattern recognition framework for PHA recognition. Section VII presents the evaluation results for the proposed STW pattern recognition framework. In

Section VIII, we perform a discussion on the potential solutions for speedup of the computing and the connection to caregivers injuries prevention. Finally, the conclusion and future work are discussed in Section IX.

II. RELATED WORK AND SENSING MODALITIES

A. Related Work on Human Activities Recognition

While the previous work in occupational safety has focused primarily on posture determination, task classification is essential for obtaining the job context for solution implementation [31]. Kim and Nussbaum classified six generic manual materials handling tasks, including box lifting, carrying, pushing, and pulling, with a precision of 90%. Although the classification was precise, the predicted task duration was typically shorter than ground truth as the classifier had difficulty in identifying the start and end time of the task [31]. In addition, the participants were required to wear 17 IMUs and 2 pressure-sensing insoles, which can interfere with task performance and would be impractical for implementation in a healthcare environment. At the other end, vision-based approaches to activity recognition using depth cameras, which require no on-body sensors, can distinguish among overhead work, lifting a load from the ground, kneeling, and crawling during construction work [21]. However, this system was similarly limited by failing to account for task repetition and, more importantly, forceful exertions, which are critical ergonomic risk factors.

Wearable sensor is another alternative approach to monitor human actions. In nursing, wearable sensors have been used to recognize activities important for staffing decisions and documentation of nursing workload [32], tracking hygiene [33], and monitoring patient care activities such as blood draws and medication distribution [33], [34]. Recognizing the importance of awkward postures in the causation of work-related injuries among nurses, recent research efforts have focused on tracking specific postures adopted by nurses [35]. This study looked at trunk postures and tracked the frequency and duration of specific extreme or awkward positions, particularly trunk inclination $>20^\circ$ and $>60^\circ$.

To date, the main research on automatically recognizing human-object interaction is based on image [36] and video [37] parsing. The camera records the process and machine learning approaches are applied to understand the scene. There is one application close to PHA recognition task, which is construction activity monitoring. The existing research study is also image and camera based [38], [39]. However, cameras are impractical in the monitoring of patient handling due to privacy concerns and technical challenges.

According to our literature research, there are no work on PHA recognition using wearable technologies.

B. Related Work on STW

Malassiotis and Strintzis [40] exploited the spatio-temporal coherence of the motion in the scene, where the displacement function is approximated by isoparametric cubic finite elements, and provide better representation of local motion. Rav-Acha *et al.* [41] proposed a new framework for STW, named evolving

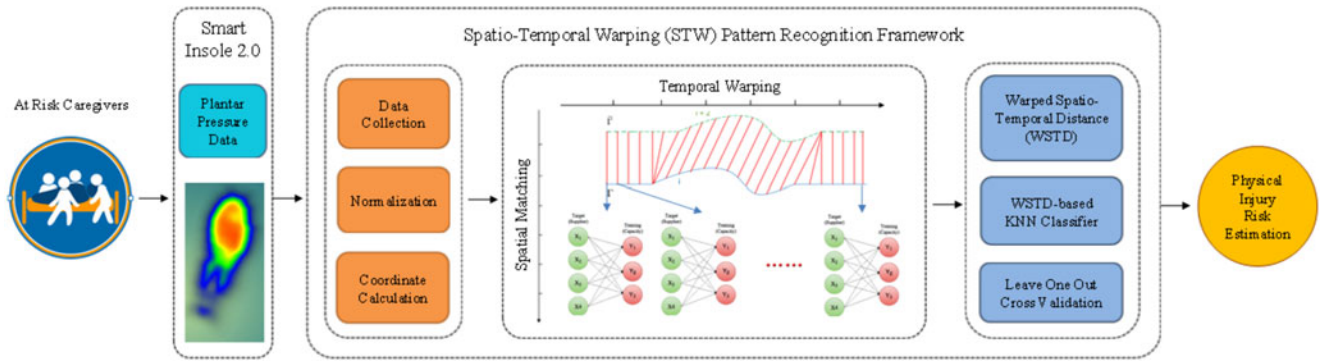


Fig. 1. Diagram of overall system design including Smart Insole 2.0 and the STW pattern recognition framework. Caregivers' activities and injury risk estimation are the input and output of the system.

the fronts, which is able to manipulate the time flow of a video sequence by sweeping an evolving time front surface through the videos aligned space-time volume. Zhou and Torre [42] proposed canonical time warping (CTW) for accurate spatio-temporal alignment between two behavioral time series to distinguish subjects performing similar activities. CTW combines canonical correlation analysis (CCA) with dynamic time warping (DTW) and it extends CCA by allowing local spatial deformations.

C. Sensing Modalities

Images and videos captured by still or video camera are popular methods to survey activities confined in a certain place. The skeleton visualization created by Kinect [43] is another visual representation. However, privacy concerns prevent these systems from being widely deployed. IMUs including accelerometer, gyroscope, and magnetometer are widely applied in activity monitoring either using one type of IMU sensor or combining multiple type sensors together. Besides, angular displacement sensor and flex sensor to measure the curvature are also used in activity recognition. However, these wearable sensors usually require high adherence from the user as binding on the arm, waist, or thigh, which causes discomfort and raise the low-compliance issue. Plantar pressure measured by piezoelectric pressure is another modality for activity recognition since both upper extremity and lower extremity exercise impose influence on the plantar pressure. To the best of our knowledge, it is the first time to employ plantar pressure for PHA recognition.

III. SYSTEM OVERVIEW

Our proposed system for PHA recognition consists of two modules including Smart Insole 2.0 and the STW framework. The diagram of this system design is shown in Fig. 1. In this design, Smart Insole 2.0 is developed acting as a sensor to collect plantar pressure during various PHAs unobtrusively. The computing of the STW framework is implemented in the smartphone. The STW framework contains a WSTD calculation including both spatial and temporal domain matching, and a WSTD-based k NN classifier, which together contribute to the similarity measurement for disparate PHAs classification. Caregivers' activities and injury risk estimation are treated as

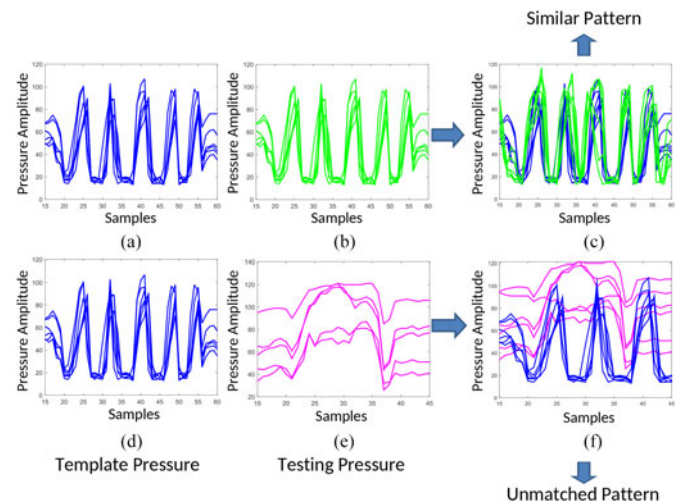


Fig. 2. Different activities show distinct patterns in terms of plantar pressure: (a) and (d) are the template samples obtained from walking. (b) is the testing sample obtained from walking performed in another trial. (e) is the testing sample obtained from bending. (c) shows same activities have similar patterns. (f) shows different activities have unmatched patterns.

input and output of the system. This system provides a sensor-rich wearable device that is capable of recognizing patient handling activities, quantifying postural demands, and identifying handling loads. This contributes a practical exposure assessment tool that can support musculoskeletal disorder prevention with minimal time requirement and cost. Accurately capturing nursing workload, has applications on identifying "best practice" for safe patient handling programs (NORA HSA Activity/Output Goal 2.2.1 [44]).

Plantar pressure variation during ambulation is employed as a unique feature for gait analysis [45], which characterizes the pressure change along the time axis. During PHAs, the plantar pressure also shows prominent patterns to differentiate among the activities, which rationalizes the utilization of such patterns for PHA recognition. Fig. 2 shows that performing same PHAs results in similar patterns while different PHAs exhibit unmatched patterns. To get a better visualization, we pick 6 out of 48 pressure sensors and show their pressure amplitude in the figure, of which each curve corresponds to a single pressure sensor. The choice of pressure sensors is described in Section

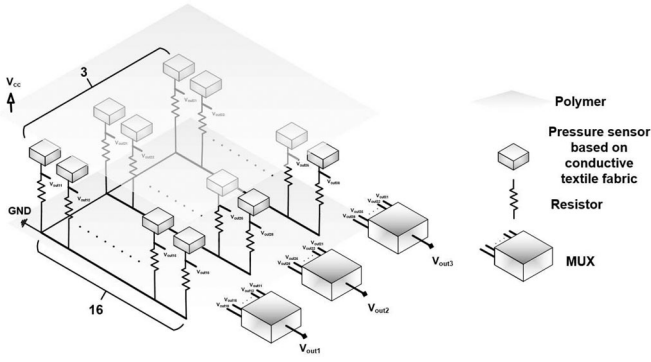


Fig. 6. Diagram of pressure sensor array circuit of Smart Insole 2.0. The output signals of pressure sensors are chosen by three 16 to 1 channel MUXs.

in Smart Insole 2.0 system, which integrates a 12-bit accelerometer, a 16-bit gyroscope, and a magnetometer in a single chip. The X - and Y -axis of magnetometer is 13-bit each and the Z -axis of magnetometer is 15-bit. The ranges of accelerometer, gyroscope, and magnetometer are ± 16 g, $\pm 2000^\circ/\text{s}$, and $2500 \mu\text{T}$, respectively. The BMX055 communicates with the MCU using an interintegrated circuit (I2C) bus. Accelerometer, gyroscope, and magnetometer data in X -, Y -, and Z -axes are sampled simultaneously.

3) Micro Control Unit and Bluetooth: The MCU and Bluetooth are implemented by a single device CC2541 from Texas Instruments [50]. The CC2541 combines a radio frequency transceiver with an enhanced 8051 MCU, a 256-kB in-system programmable flash memory, an 8-kB random-access memory, a 12-bit ADC, and a hardware I2C bus. The sensor data from three MUXs are digitalized by eight-channel, 12-bit, and 0-3.3 volt ADC module. The sampling rate can be adaptive for specific applications, up to 100 samples/s (Hz).

4) Battery and MicroUSB Connector: The battery module contains a battery connector, a 3.3-V low-dropout regulator (XC6206-3.3), a system power switch (SI2301), and a metal-oxide-semiconductor field-effect transistor (MOSFET). The MOSFET is controlled by the MCU for connecting and disconnecting power for nine-axis inertial sensor and channel MUXs. The microUSB connector is used for charging battery, programming CC2541, and online debugging.

5) Package and Ergonomic Design: Smart Insole 2.0 is lightweight (< 2 oz.), thin, and convenient to use. It is well packed that there are two layers on top of the pressure sensors and circuits. First, one layer made of waterproof polymer is to prevent water from permeating down to the sensor and circuit area. On top of it there is another water absorbing layer made of fabric, so little sweat or water will not impact the performance of the insole. It also does not need calibration and only requires minimal setup procedures. The package of Smart Insole 2.0 is shown in Fig. 4(b). Smart Insole 2.0 is similar to a normal insole without any extra cable, antenna, or adhesive equipment.

B. Software Stacks and Visualization

The software system on the smartphone for Smart Insole 2.0 is shown in Fig. 7(a). In order to perform the real-time computing,

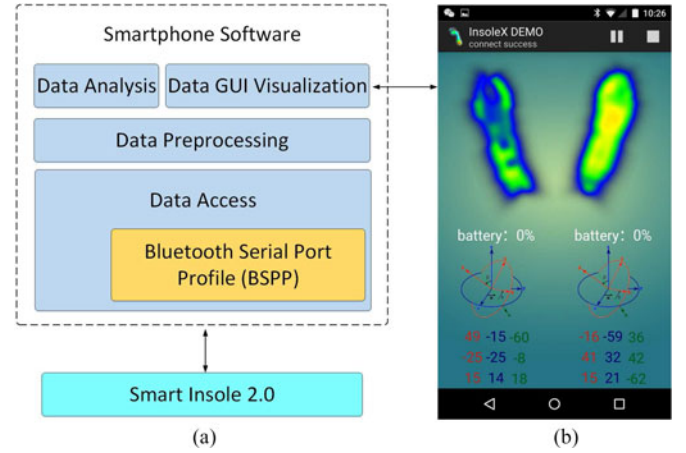


Fig. 7. Software system on the smartphone. (a) Stacked software structure. (b) Data GUI visualization.

the software is implemented with multithreading technology. In general, there are four main threads in the software program including data access, data preprocessing, data analysis, and data graphic user interface (GUI) visualization. Specifically, the data access thread handles asynchronous communication to Smart Insole 2.0 over the Bluetooth serial port profile. The thread synchronizes the incoming sensor data before forwarding to the client programs over interconnect sockets. Data preprocessing thread performs data preprocessing, including de-noising of the collected pressure sensor data [48], calibrating inertial sensor values with filtering, and initializing the baseline with magnetometer data. After the above steps, the clean, compressive, and informative data are obtained. After that the following processing will be dispatched to the corresponding services on the next layer. Data analysis is the core part in the software, and it will analyze the streamed data from insole. In this specific application, it will recognize the activities of patient handling. The detail of this thread will be presented in Section V. Data GUI visualization has been developed to record, visualize, and analyze the data from Smart Insole 2.0, as shown in Fig. 7(b). The data are transmitted to the smartphone from Smart Insole 2.0 via Bluetooth, and stored in the memory of the smartphone.

V. WARPED SPATIO-TEMPORAL DISTANCE

Suppose we have two high-dimensional time series Γ and $\tilde{\Gamma}$

$$\Gamma = \{\gamma_1, \gamma_2, \dots, \gamma_m, \dots, \gamma_M\}, \quad (1)$$

$$\tilde{\Gamma} = \{\tilde{\gamma}_1, \tilde{\gamma}_2, \dots, \tilde{\gamma}_n, \dots, \tilde{\gamma}_N\} \quad (2)$$

where M and N are the sample sizes, γ_m and $\tilde{\gamma}_n$ can be represented as

$$\gamma_m = \{p_1^m, p_2^m, \dots, p_j^m, \dots, p_{N_p}^m\}^T, \quad (3)$$

$$\tilde{\gamma}_n = \{\tilde{p}_1^n, \tilde{p}_2^n, \dots, \tilde{p}_k^n, \dots, \tilde{p}_{\tilde{N}_p}^n\}^T \quad (4)$$

where N_p and \tilde{N}_p are the dimensions of γ_m and $\tilde{\gamma}_n$, respectively.

In spatial domain, for each pair of γ_m and $\widetilde{\gamma}_n$, the data are normalized as

$$q_j^m = \frac{p_j^m}{\sum_{j=1}^{N_p} p_j^m}, \quad (5)$$

$$\widetilde{q}_k^n = \frac{\widetilde{p}_k^n}{\sum_{k=1}^{\widetilde{N}_p} \widetilde{p}_k^n}. \quad (6)$$

Then, we define the cost c_{jk} of transporting between j th data from γ_m , which is q_j^m , and k th data from $\widetilde{\gamma}_n$, which is \widetilde{q}_k^n . The definition of cost depends on the specific applications. Some examples include Euclidean distance and Taxicab distance.

The next task is to find a flow, $\mathbf{F}(j, k) = f_{jk}$, such that the matching work between two datasets γ_m and $\widetilde{\gamma}_n$ will have the least cost [51]:

$$\min \sum_{j=1}^{N_p} \sum_{k=1}^{\widetilde{N}_p} c_{jk} f_{jk} \quad (7)$$

subject to

$$\sum_{j=1}^{N_p} q_j^m = \sum_{k=1}^{\widetilde{N}_p} \widetilde{q}_k^n, \quad (8)$$

$$f_{jk} \geq 0, 1 \leq j \leq N_p, 1 \leq k \leq \widetilde{N}_p, \quad (9)$$

$$\sum_{k=1}^{\widetilde{N}_p} f_{jk} \leq q_j^m, 1 \leq j \leq N_p, \quad (10)$$

$$\sum_{j=1}^{N_p} f_{jk} \leq \widetilde{q}_k^n, 1 \leq k \leq \widetilde{N}_p, \quad (11)$$

$$\sum_{j=1}^{N_p} \sum_{k=1}^{\widetilde{N}_p} f_{jk} = \min \left(\sum_{j=1}^{N_p} q_j^m, \sum_{k=1}^{\widetilde{N}_p} \widetilde{q}_k^n \right). \quad (12)$$

Once the above problem is solved, and we have found the optimal flow \mathbf{F} , the spatial warping (SW) metric is found as the matching work normalized by the total flow as follows:

$$\text{SW}(\gamma_m, \widetilde{\gamma}_n) = \text{SW}(\widetilde{\gamma}_n, \gamma_m) = \frac{\sum_{j=1}^{N_p} \sum_{k=1}^{\widetilde{N}_p} c_{jk} f_{jk}}{\sum_{j=1}^{N_p} \sum_{k=1}^{\widetilde{N}_p} f_{jk}}. \quad (13)$$

In temporal domain, to measure the similarity between these two high-dimensional time series Γ and Γ_i , an $N \times M$ matrix \mathbf{D} is created, called *distance matrix*. The value of the $(n$ th, m th) element in \mathbf{D} represents the distance $d(\widetilde{\gamma}_n, \gamma_m)$ between high-dimensional points $\widetilde{\gamma}_n$ and γ_m , as shown below:

$$\mathbf{D}(n, m) = d(\widetilde{\gamma}_n, \gamma_m) \quad (14)$$

where SW defined in (13) is adopted as the distance metric, so we obtain

$$\mathbf{D}(n, m) = \text{SW}(\widetilde{\gamma}_n, \gamma_m). \quad (15)$$

With help of the distance matrix, the shortest warped path through the matrix can be derived [52]:

$$cd(n, m) = \text{SW}(\widetilde{\gamma}_n, \gamma_m) + \min \begin{cases} cd(n, m-1) \\ cd(n-1, m) \\ cd(n-1, m-1) \end{cases} \quad (16)$$

$$1 \leq n \leq N, 1 \leq m \leq M$$

where $cd(n, m)$ is the current minimum cumulative distance for $\mathbf{D}(n, m)$, and the initial setting is $cd(0, 0) = 0, cd(0, m) = cd(n, 0) = \infty$.

After that, the overall minimized cumulative distance $cd(N, M)$ can be found. Finally, the WSTD is calculated as below:

$$\text{WSTD} = \sqrt{cd(N, M)}. \quad (17)$$

The whole operation procedure of WSTD calculation is summarized in Algorithm 1 named WSTD.

Algorithm 1: Warped Spatio-Temporal Distance.

```

1: Input: high-dimensional time series  $\Gamma$  and  $\widetilde{\Gamma}$ ;
2: Initial:
3:  $cd(0, 0) = 0, cd(0, m) = cd(n, 0) = \infty$ ;
4: for  $m = 1 : M$  do
5:   for  $n = 1 : N$  do
6:     for  $j = 1 : N_p$  do
7:        $q_j^m \leftarrow p_j^m$ ; //Normalization
8:     end for
9:     for  $k = 1 : \widetilde{N}_p$  do
10:       $\widetilde{q}_k^n \leftarrow \widetilde{p}_k^n$ ; //Normalization
11:    end for
12:     $c_{jk}$  //Cost Calculation
13:     $F_{jk} \leftarrow \min \sum_{j=1}^{N_p} \sum_{k=1}^{\widetilde{N}_p} c_{jk} f_{jk}$ ; // (7)–(12)
14:     $\text{SW}(\gamma_m, \widetilde{\gamma}_n) \leftarrow c_{jk}, F_{jk}$ ;
15:     $\mathbf{D}(n, m) \leftarrow \text{SW}(\gamma_m, \widetilde{\gamma}_n)$ ;
16:     $cd(n, m) \leftarrow \begin{cases} \mathbf{D}(n, m) \\ \min \begin{cases} cd(n, m-1) \\ cd(n-1, m) \\ cd(n-1, m-1); \end{cases} \end{cases}$ 
// (15), (16)
17:   end for
18: end for
19:  $cd(N, M)$ ;
20:  $\text{WSTD} \leftarrow cd(N, M)$ ;
21: Output:  $\text{WSTD}$ .
    
```

VI. PHA RECOGNITION FRAMEWORK

In this section, we will present the STW pattern recognition framework for PHA recognition including WSTD-based pressure pattern recognition and a WSTD-based k NN classifier.

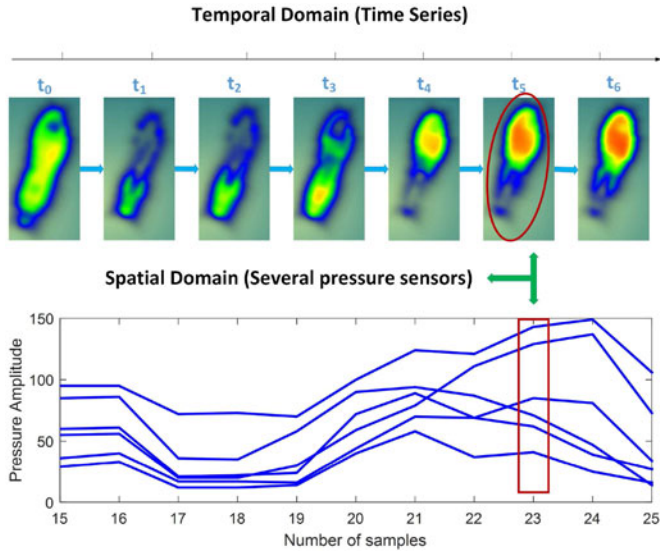


Fig. 8. Spatio-temporal matching in a walking while pushing wheelchair forward activity. For better visual effect, we only show six channels pressure waveforms in the lower part of this figure.

A. Framework Foundation

The study proposed in this project is motivated by the observation that most of patient handling activities and body postures can be associated with characteristic spatio-temporal pressure patterns under foot. Patient handling and movement activities [35], [53] are the tasks involving transfer of a load or patient. Safe PHAs follow standardized procedure in order to prevent the risk to the caregivers' lumbar spine and injury to the patient. Vibrations, changes in center of gravity, balance shifts, and even hand motions can propagate throughout the entire body to influence the pressure distribution of the feet on the ground. For example, the pressure distribution of the feet when the caregiver is standing in front of the patient bed is different from when she is reaching and turning a heavy patient from the other side. In the temporal domain, the plantar pressure can be modeled as a bunch of time series along the period of patient handling. The basic principle of temporal matching is to allow two time series that are similar, but locally out of phase, to align in a nonlinear manner by warping the time axis iteratively until an optimal match (according to a suitable metric) between the two sequences is found [54]. Therefore, it is able to handle subjects with different walking speed. In the spatial domain, the plantar pressure is distributed in different locations including toe, metatarsal, and heel area. As a result, the pressure variation occurs among the pressure points distributed in the whole foot area and in different stages of the activity, which shows the spatio-temporal nature of plantar pressure during activities.

B. Spatio-Temporal Characteristics of Plantar Pressure

The plantar pressure during activities exhibits spatial-temporal characteristics. For example, the diagram of pressure in spatial-temporal distribution in a walking while pushing wheelchair forward activity is shown in Fig. 8. In t_0 , the subject stands still. Starting from t_1 , the subject begins to walk ahead.

As time elapses, the pressure changes along the temporal axis. As shown in Fig. 8, when heel-strike happens, the pressure in heel area increases, followed by a pressure increase in toe area leading to toe-off. In each time stamp t_i , the spatial domain data are plantar pressure collected from 48 pressure points, as shown in Fig. 5, covering the whole foot area. For better visual effect, we only show six channels pressure waveforms in the lower part of Fig. 8.

After completing the spatial-temporal matching, a WSTD is obtained to quantify the similarity between two activities.

C. WSTD-Based Pattern Recognition

Let $z(t)$ be the continuous-time sensed pressure data and T_s be the sampling period. The discrete pressure sample in each pressure sensor can be written as

$$z_i = z(iT_s). \quad (18)$$

Assuming each pressure sensor in Smart Insole 2.0 is sampled N_s times, the total pressure data can be represented in the form of (1) as

$$\Gamma_z = \{\gamma_1, \gamma_2, \dots, \gamma_i, \dots, \gamma_{N_s}\}, \quad (19)$$

$$\gamma_i = \{z_1^i, z_2^i, \dots, z_l^i, \dots, z_{N_{pr}}^i\}^T \quad (20)$$

where γ_i is a vector containing all the pressure data in the i th sampling, z_l^i is the pressure from l th sensor in i th sampling, and N_{pr} is the number of pressure sensors used in the insole.

Suppose Γ_z is the training data, $\tilde{\Gamma}_z$ is the testing data defined similar to (2). The sample size of $\tilde{\Gamma}_z$ is \tilde{N}_s and the number of pressure sensors is also N_{pr} .

The Euclidean distance is adopted as the $cost = c_{jk}$ between each training and testing pair as

$$c_{jk} = \sqrt{(X_j - \tilde{X}_k)^2 + (Y_j - \tilde{Y}_k)^2} \quad (21)$$

where (X_j, Y_j) and $(\tilde{X}_k, \tilde{Y}_k)$ represent the coordinates of the pressure points in the insole of training set and testing set, respectively. The choice of Euclidean distance is because the pressure is distributed in a 2-D plane.

Then, we apply Algorithm 1 to the pressure data by taking Γ_z and $\tilde{\Gamma}_z$ as Γ and $\tilde{\Gamma}$, respectively. After completion of Algorithm 1, we can obtain the WSTD between the training data and testing data of the plantar pressure.

The Sakoe-Chiba [55] band is used to constrain the warping path for speeding up the temporal domain calculation. The most important parameter of this method is the constraint R , which is defined as the rate of the warping length over the whole sequence, and it varies from 0 to 100%. Considering the fact that our pressure data for different activities are unsynchronized, the unique pattern corresponding to each activity may appear in arbitrary position of the pressure sequence. In addition, the data lengths of each activity are usually different because the time spent on a PHA for a subject is arbitrary in real life. In order to tolerate the mismatch gap as big as possible, we do not impose

a constraint on the warping path. Therefore, R is set as 100% in our framework.

D. WSTD-Based k NN Classifier

k -nearest neighbors embedding with WSTD forms the PHA classifier. In this classifier, an object is classified by a majority vote of its neighbors with the object being assigned to the class most common among its k nearest neighbors, in which the nearest neighbors are determined by the aforementioned WSTD between them rather than using the Euclidean distance.

VII. EVALUATION

A. Experimental Setup

We ran a series of experiments in a laboratory environment to evaluate the performance of our proposed spatial-temporal framework for PHA recognition. The dataset is collected by our Smart Insole 2.0 from eight subjects including seven male subjects and one female subject.¹¹ The weights of all participants are from 58 to 85 kg and heights from 160 to 185 cm. Each subject performed eight different PHAs [35], [53] including: 1) *bend to lift an item from floor level*; 2) *stand while lifting patients leg*; 3) *stand while lifting patient from wheelchair*; 4) *stand while rolling patient*; 5) *sit normally*; 6) *walk normally*; 7) *walk while pushing wheelchair forward*; 8) *walk with both hands carrying a chair*. To be specific, in 2), the subject lifts a patient's leg and keeps for 3 s then slowly puts down the leg. Likewise, in 4), the subject rolls over a patient and also keeps for 3 s then rolls back to the original position. In 8), the subject first lifts the wheelchair up then walks forward with two hands carrying the wheelchair. The real experimental scenes are shown in Fig. 9.

In the data collection protocol, each activity was completed within 6 s which correspond to 90 samples. Two seconds period corresponding to 30 samples were used as guard interval for the subject preparing for the next activity such as turning around or getting proper position ready to perform the action. Therefore, the data from each pressure sensor were segmented every 120 samples with the first 90 effective samples used for the patient handling activities recognition and the rest 30 samples ignored. The length of each segment is 120 samples.

B. Quantitative Evaluation in a Controlled Study

For this part, we evaluate the classification performance of our proposed framework. A leave-one-out cross-validation is adopted to quantify the accuracy. Specifically, the whole dataset is divided into two sets. One observation is selected as the validation set and the remaining observations as the training set. The whole procedure requires to learn and validate N_{cv} times, where N_{cv} is the number of observations in the original sample. In this quantitative evaluation, each subject is required to perform 10 trials on each activity. Therefore, N_{cv} equals to 640 in our case.

¹¹Our team holds an active IRB protocol in the State University of New York at Buffalo (#: 695026-2), which allows for recording motion through wearable sensors while performing patient handling activities.

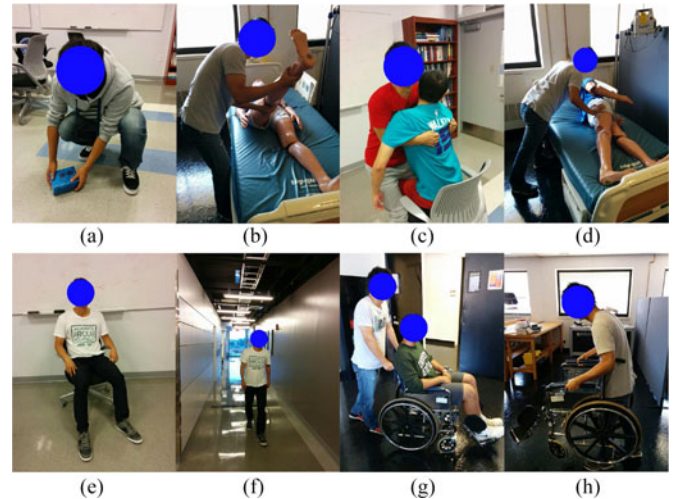


Fig. 9. Eight different PHAs performed in experiments including: (a) Bend leg to lift an item from floor level. (b) Stand while lifting patient's leg. (c) Stand while lifting patient from wheelchair. (d) Stand while rolling patient. (e) Sit normally. (f) Walk normally. (g) Walk while pushing wheelchair forward. (h) Walk with both hands carrying a chair.

1) **Pressure Data Visualization:** The spatial-temporal pressure data and 3-D visualization are shown in Fig. 10. In each sub-figure, top one is the 3-D representation and bottom one is the raw pressure data. Since we observed that the curves with all 48 channels data from Smart Insole 2.0 in one figure makes the pressure variation pattern too dense to be seen clearly, we pick six out of 48 pressure points and show their waveforms for a better visualization. The choice of the six pressure points are Number 1, 11, 22, 32, 39, and 47 marked on Smart Insole 2.0, as shown in Fig. 10(i). The order of the six pressure points corresponds to the order of sensor ID in the 3-D visualization part with the lines between two sub-figures showing the one-to-one relationship.

Take a closer look at the waveforms in Fig. 10, each sub-figure shows discriminating pattern affiliated with different PHAs. Among them, (f) *walk normally*; (g) *walk while pushing wheelchair forward*; and (h) *walk with both hands carrying a chair* are all walking-based activities, which exhibit similarity in some extent, because they all possess pseudo-periodic nature in ambulation. However, the differences among them are still noticeable to distinguish these three activities. In *walk with both hands carrying a chair*, before walking, the subject needs to lift the chair first, such lifting behavior causes prominent pressure fluctuation at the beginning of the time series data which makes itself a unique identifier of such activity. For comparison between *walk normally* and *walk while pushing wheelchair forward*, we notice that walking normally has higher average pressure amplitude than walking while pushing wheelchair forward. Meanwhile, the data obtained from *walk while pushing wheelchair forward* in different sensor locations have less variability than those obtained from *walk normally*. This phenomenon is due to that part of the body weight is shared by the handle of the wheelchair when the subject holds it to push the wheelchair forward. For comparison between (b) *stand while*

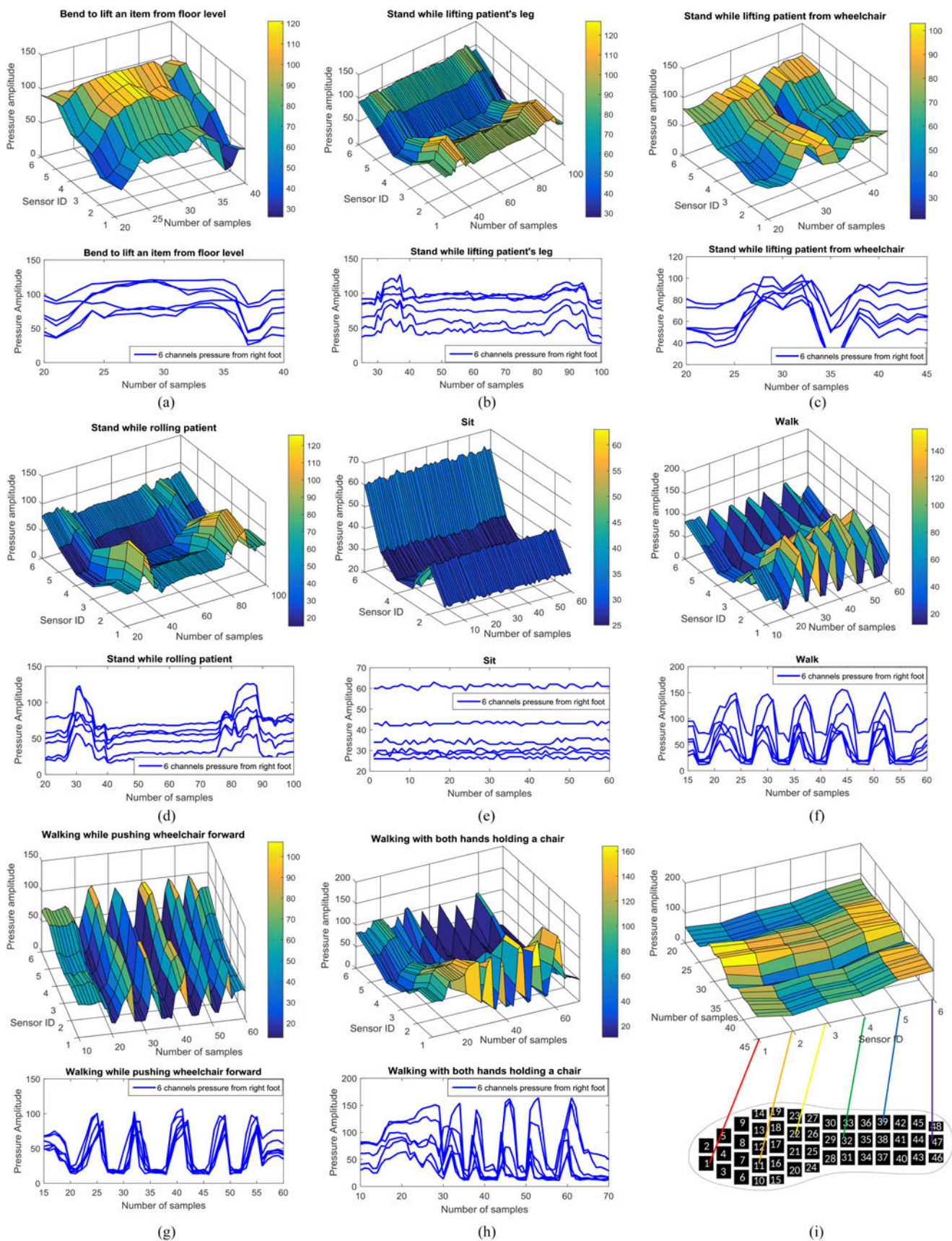


Fig. 10. Spatial-temporal pressure data and 3-D visualization from Smart Insole 2.0: (a) Bend to lift an item from floor level. (b) Stand while lifting patients leg. (c) Stand while lifting patient from wheelchair. (d) Stand while rolling patient. (e) Sit normally. (f) Walk normally. (g) Walk while pushing wheelchair forward. (h) Walk with both hands carrying a chair. (i) Pressure points selection and matching.

TABLE I
CONFUSION TABLE OF RECOGNITION ON 8 PHAS USING 48 PRESSURE SENSORS

	a	b	c	d	e	f	g	h	Total	Recall (Sensitivity)
a	80	0	0	0	0	0	0	0	80	100%
b	0	72	6	2	0	0	0	0	80	90%
c	7	2	70	0	0	1	0	0	80	87.5%
d	0	5	2	73	0	0	0	0	80	91.3%
e	0	0	0	0	80	0	0	0	80	100%
f	3	0	0	0	0	76	1	0	80	95%
g	0	0	3	0	0	6	71	0	80	88.8%
h	1	0	3	0	0	4	7	65	80	81.3%
Total	91	79	84	75	80	87	79	65		
Precision	87.9%	91.1%	83.3%	97.3%	100%	87.4%	89.9%	100%		
Specificity	98.0%	98.8%	97.5%	99.6%	100%	98.0%	98.6%	100%		

TABLE II
CATEGORIZATION OF PHA INTO HIGH LEVEL ACTIVITIES

Activity category	Activities description
a	Stand
b	Bend to lift an item from floor level
c	Stand while lifting patients leg
d	Stand while lifting patient from wheelchair
e	Stand while rolling patient
f	Sit
g	Sit normally
h	Walk
	Walk normally
	Walk while pushing wheelchair forward
	Walk with both hands carrying a chair

lifting patients leg and (d) stand while rolling patient, we observe that the pressure changing peaks in stand while rolling patient are steeper than the ones in stand while lifting patients leg, because the load imposed by rolling a body is heavier than lifting a leg.

2) Accuracy Evaluation: The quantitative evaluation performance is measured by classification accuracy. Given the large number of testing inquiries, the framework should offer the correct responses with high probability. The accuracy (ACC) is defined as

$$ACC (\%) = \frac{TP + TN}{P + N} \times 100\% \quad (22)$$

where TP represents the true positive, TN represents the true negative, P represents the positive, and N represents the negative. In injury risk estimation, qualitative profile recognition, PHA recognition, and load estimation are three key parameters [56]. PHA recognition is used for estimating injury probability for each PHA. Qualitative profile recognition and load estimation are used in estimating workload and load in performing PHA, respectively.

a) Qualitative Profile Recognition: Qualitative profile recognition is used to estimate the workload in a nursing environment. Based on the percentages of all-body activities (i.e., walk related), upper-body activities (i.e., standing related), and break (i.e., sitting) in a working period, we can infer the intensity level of the workload. Here, all the aforementioned eight PHAs are categorized into three qualitative profiles as described in Table II, which facilitates the workload estimation. First

TABLE III
CONFUSION TABLE OF RECOGNITION ON THREE CATEGORIZED ACTIVITIES

	Stand (a, b, c, d)	Sit (e)	Walk (f, g, h)	Total	Recall
Stand (a, b, c, d)	319	0	1	320	99.7%
Sit (e)	0	80	0	80	100%
Walk (f, g, h)	10	0	230	240	95.8%
Total	329	80	231		
Precision	97.0%	100%	99.6%		

profile is stand including bend to lift an item from floor level; stand while lifting patients leg; stand while lifting patient from wheelchair; and stand while rolling patient. Second profile is sit including sit normally, and third profile is walk including walk normally; walk while pushing wheelchair forward; and walk with both hands carrying a chair. Both recall and precision achieve more than 95.8% as shown in Table III. The overall accuracy is 98.3%, which shows high performance of qualitative profile recognition. Note that the performance from qualitative profile recognition is better than the one with PHA recognition, which is because several confusing activities actually belong to the same qualitative profile such as stand or walk. In such case, these PHAs are treated as no difference in terms of qualitative profile. The qualitative profile recognition can be further applied in other workplaces such as construction industry and wholesale and retail trades [57].

b) PHA Recognition: The goal of PHA recognition is to accurately classify each PHA defined in Fig. 9. Table I shows the confusion table with respect to PHA classification using 48 pressure sensors. The overall accuracy is 91.7%. We notice that the activity walk with both hands carrying a chair has the lowest recall rate 81.3%, which is often confused with walk normally and walk while pushing wheelchair forward. The reason of this is that all the three activities are performed in walking status, in which the pressure obtained from them all shows similar pseudo-periodic nature, as shown in Fig. 10. This accuracy can be further improved by analyzing IMU data together with pressure data. The remaining seven recall rates are above 87.5%. Specifically, sit reaches 100% recall and 100% precision because of the minimal fluctuation it exposed that differentiates it from other activities. In terms of precision, stand while lifting patient from wheelchair shows the lowest rate of 83.3% because the data

TABLE IV
CATEGORIZATION OF PHA INTO LOAD LEVELS

Load levels	Activities description	
c	Heavy	Stand while rolling patient
d		Stand while lifting patient from wheelchair
h		Walk with both hands carrying a chair
a	Light	Bend to lift an item from floor level
b		Stand while lifting patients leg
g		Walk while pushing wheelchair forward
e	No	Sit normally
f		Walk normally

TABLE V
CONFUSION TABLE OF RECOGNITION ON THREE CATEGORIZED LOAD LEVELS

	Heavy (c, d, h)	Light (a, b, g)	No (e, f)	Total	Recall
Heavy (c, d, h)	213	22	5	240	88.8%
Light (a, b, g)	11	223	6	240	92.9%
No (e, f)	0	4	156	160	97.5%
Total	224	249	167		
Precision	95.1%	89.6%	93.4%		

from other activities show similarity to the data of *stand while lifting patient from wheelchair* leading to mis-classification.

c) Load Estimation: The load estimation is to estimate the load imposed on caregivers when they perform certain PHA. To be specific, *stand while lifting patient from wheelchair*, *stand while rolling patient*, and *walk with both hands carrying a chair* are categorized as *heavy load* because caregivers need to use more force when performing such PHAs. *Bend to lift an item from floor level*, *stand while lifting patients leg*, and *walk while pushing wheelchair forward* are considered as *light load* as these activities involve moderate force exertion. *Sit normally* and *walk normally* are considered as *no load* as they are performed without external load. The grouping criterion depends on the specific ongoing activity. Note that we decide *bend to lift an item from floor level* as *light load* because that item the subject picked up indicates the specific weight of the object in our experiment. The load level category is summarized in Table IV. Likewise, the confusion table with respect to load levels is shown in Table V. The overall accuracy is 92.5%. *Heavy load* has the lowest recall of 88.8%, in which 22 activities are mis-classified as *light load*. Since these two load level both involve forceful exertion, they may be confused with each other.

3) Investigation on Sensor Dimension Reduction: In this experiment, we investigate the impact of pressure sensor number to the algorithm performance, which is measured by balanced accuracy (BAC). BAC is defined as the average of the sensitivity and the specificity as

$$\text{BAC (\%)} = \frac{\text{Sensitivity} + \text{Specificity}}{2} \quad (23)$$

or the average accuracy obtained on either class [58], which avoids inflated performance estimates on imbalanced datasets.

Balanced accuracy comparison with different sensor number

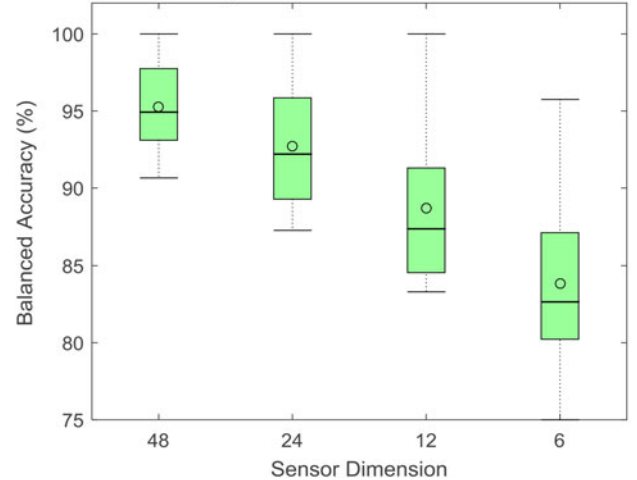


Fig. 11. Impact of sensor dimension on BAC.

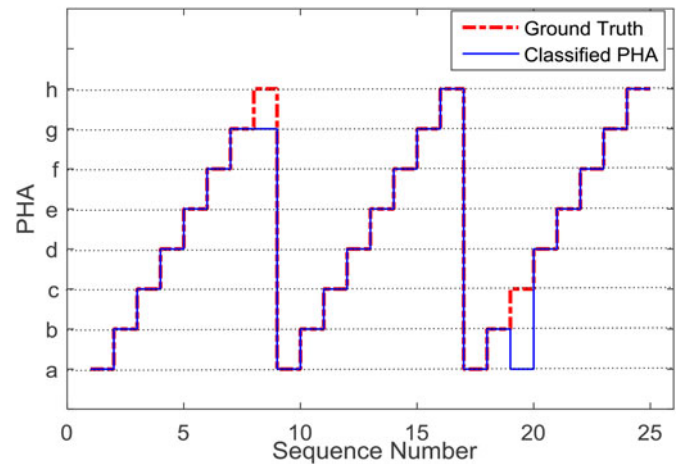


Fig. 12. Set of eight PHAs performed sequentially against ground truth.

The default sensor number is 48 including all the sensors in Smart Insole 2.0, and all the above results are obtained with this configuration. Now, we start reducing the numbers by dividing two until the sensor number reaches 6. Fig. 11 shows the BAC result in terms of sensor number. We notice that the BAC decrease with the decrement of sensor number, which implies the spatial diversity is not fully explored in reduced sensor cases.

C. Evaluation of a Longitudinal Pilot Study

As a further evaluation of this spatial-temporal framework for PHA recognition in real life, we carried out a longitudinal study of continuous monitoring through a number of aforementioned PHAs. More specifically, each of the eight activities was performed sequentially to test whether the proposed framework can classify them correctly. Fig. 12 shows the evaluation result, where the red dash line indicates the ground truth, and the blue line indicates the actual classification outcome. We observed that only two out of 24 activities are mis-classified.

VIII. DISCUSSION

A. Computing Time

The actual computing time is related to the number of pressure sensors. As stated in Section VI, N_{pr} is the number of pressure sensors used in the insole. After applying Algorithm 1 to the training and testing data, N_p and \widetilde{N}_p in STW framework are both instantiated as N_{pr} in the Section VI. As a result, N_p and \widetilde{N}_p equal to the number of pressure sensors. Also as seen from (7) to (13), N_p and \widetilde{N}_p are directly related to the WSTD calculation. So that is the reason that the algorithm computing cost relates to the number of pressure sensors.

In theory, the WSTD algorithm is computationally costly because the distance calculation has no close form solution yet. Specifically, its worst case time complexity is $O(n^5 \log n)$ where the spatial matching is $O(n^3 \log n)$ and the temporal warping is $O(n^2)$. There are considerable works on reducing the complexity of earth mover's distance (EMD) and DTW by approximation. For example, in spatial matching, the worst case computing cost can be reduced to approximately 50% by applying the preprocessing procedure of EMD [59]. In temporal matching, the Sakoe-Chiba band optimization method [60] used in DTW can be applied to speed up the temporal warping by adjusting the constraint R , whereas the recognition performance will be sacrificed in some extent. In such circumstance, a better tradeoff between accuracy performance and computing speed is required. Furthermore, the lower bound optimization method used in DTW can achieve additional 10–50× speedup for temporal matching [61]. Note that in our application, the analysis is performed in nonreal time, and the processing algorithm is implemented in the back.

B. Connection to Caregivers Injuries Prevention

Our system can contribute to caregiver injury reduction in multifaceted aspects. First, there are many solid facts that most of nurses suffered chronic occupational diseases such as musculoskeletal disorders, low back pain and shoulder pain due to awkward body postures, overexertion and long-term fatigue [6]. It is critical to monitor their work routine and estimate the possible injury risk. Smart Insole and the proposed STW framework can serve as a cost-effective practical exposure assessment tool for healthcare workers to provide a set of qualitative profile, patient handling activities, and load recognition, where qualitative profile with work duration contributes to long-term fatigue, patient handling activities contributes to awkward body posture, and load estimation contributes to overexertion, respectively. Our results can help nurses to monitor their working action in long-term and guide the correct patient handling to avoid unprofessional actions. Second, nurses workload is diverse and event-driven. Particularly, some awkward postures, such as rolling/carrying a patient [35], are ad hoc according to the need in the field. It is necessary to perform the monitoring during their daily workspan. Third, for the purpose of nurse or nursing students training, currently, the best practice of exposure assessment often relies on visual inspection performed by an

observer [13]. Our system holds the potential to transform the current episodic, subjective observation-based approach into a continuous, unobtrusive and objective measurement-based method in monitoring caregivers and nursing workforce.

IX. CONCLUSION AND FUTURE WORK

To accurately recognize the PHA, we first developed Smart Insole 2.0 to capture the plantar pressure change information caused by the PHA. A WSTD algorithm and a WSTD-based recognition framework were proposed to analyze the pressure data for classification. The experimental results showed that our framework can achieve 91.7% overall accuracy with eight different PHAs. Meanwhile, the qualitative profile and load level can also be classified with accuracies of 98.3% and 92.5%, respectively. Moreover, we also discussed the influence of sensor numbers, which shows that the performance decreases with the reduction of sensor numbers. On the other hand, the computing cost is also decreased which will speed up the WSTD algorithm.

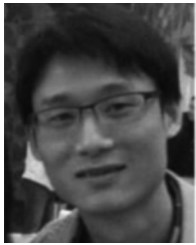
In the future, the system will be further enhanced in the following aspects. First, in this WSTD-based PHA recognition, we only use pressure information from Smart Insole 2.0. IMU data can be employed as additional features to help recognize the activities which will be a promising research direction in the future work. Second, a larger cohort will be included for a large population test.

REFERENCES

- [1] Bureau of Labor Statistics, US Department of Labor. (2015, May). Occupational employment and wages. animal control workers (33-9011). last accessed April 5 2016. [Online]. Available: <http://www.bls.gov/oes/current/oes339011.htm>
- [2] Bureau of Labor Statistics, US Department of Labor. (2011, Nov.). Table R8. Incidence rates for nonfatal occupational injuries and illnesses involving days away from work per 10,000 full-time workers by industry and selected events or exposures leading to injury or illness. last accessed April 5 2016. [Online]. Available: <http://www.bls.gov/iif/oshwc/osh/case/ostb2832.txt>.
- [3] Bureau of Labor Statistics, US Department of Labor. (2015, Nov.). Non-fatal occupational injuries and illnesses requiring days away from work, 2014. last accessed April 5 2016. [Online]. Available: <http://www.bls.gov/news.release/pdf/osh2.pdf>
- [4] K. Siddharthan, M. Hodgson, D. Rosenberg, D. Haiduven, and A. Nelson, "Under-reporting of work-related musculoskeletal disorders in the veterans administration," *Int. J. Health Care Quality Assurance*, vol. 19, no. 6, pp. 463–476, 2006.
- [5] American Nurses Association. (2011). ANA Health & Safety Survey: Hazards of the RN Work Environment. last accessed April 5 2016. [Online]. Available: <http://nursingworld.org/FunctionalMenuCategories/MediaResources/MediaBackgrounders/The-Nurse-Work-Environment-2011-Health-Safety-Survey.pdf>
- [6] (2013, Oct.). Work-Related Musculoskeletal Disorders (WMSDs) Prevention. last accessed April 5 2016. [Online]. Available: <http://www.cdc.gov/workplacehealthpromotion/evaluation/topics/disorders.html>
- [7] L. J. Hayes *et al.*, "Nurse turnover: A literature review," *Int. J. Nursing Stud.*, vol. 43, no. 2, pp. 237–263, 2006.
- [8] C. I. MacKusick and P. Minick, "Why are nurses leaving? findings from an initial qualitative study on nursing attrition," *Medsurg Nursing*, vol. 19, no. 6, pp. 335–340, 2010.
- [9] T. R. Waters and K. Rockefeller, "Safe patient handling for rehabilitation professionals," *Rehabil. Nursing*, vol. 35, no. 5, pp. 216–222, 2010.
- [10] C. C. Caruso and T. R. Waters, "A review of work schedule issues and musculoskeletal disorders with an emphasis on the healthcare sector," *Ind. Health*, vol. 46, no. 6, pp. 523–534, 2008.

- [11] S. Kim and M. A. Nussbaum, "Performance evaluation of a wearable inertial motion capture system for capturing physical exposures during manual material handling tasks," *Ergonomics*, vol. 56, no. 2, pp. 314–326, 2013.
- [12] S. E. Mathiassen, P. Liv, and J. Wahlström, "Cost-efficient measurement strategies for posture observations based on video recordings," *Appl. Ergonom.*, vol. 44, no. 4, pp. 609–617, 2013.
- [13] V. L. Paquet, L. Punnett, and B. Buchholz, "Validity of fixed-interval observations for postural assessment in construction work," *Appl. Ergonom.*, vol. 32, no. 3, pp. 215–224, 2001.
- [14] S. Gallagher and J. R. Heberger, "Examining the interaction of force and repetition on musculoskeletal disorder risk: a systematic literature review," *Human Factors: J. Human Factors Ergonom. Soc.*, vol. 55, no. 1, pp. 108–124, 2013.
- [15] A. Garg and J. M. Kapellusch, "Applications of biomechanics for prevention of work-related musculoskeletal disorders," *Ergonomics*, vol. 52, no. 1, pp. 36–59, 2009.
- [16] L. A. Cavuoto and M. A. Nussbaum, "Influences of obesity on job demands and worker capacity," *Current Obesity Rep.*, vol. 3, no. 3, pp. 341–347, 2014.
- [17] T. Waters, J. Collins, T. Galinsky, and C. Caruso, "NIOSH research efforts to prevent musculoskeletal disorders in the healthcare industry," *Orthopaedic Nursing*, vol. 25, no. 6, pp. 380–389, 2006.
- [18] A. Garg, B. Owen, and B. Carlson, "An ergonomic evaluation of nursing assistants' job in a nursing home," *Ergonomics*, vol. 35, no. 9, pp. 979–995, 1992.
- [19] D. Chen, J. Yang, and H. D. Wactlar, "Towards automatic analysis of social interaction patterns in a nursing home environment from video," in *Proc. 6th ACM SIGMM Int. Workshop Multimedia Inf. Retrieval*, 2004, pp. 283–290.
- [20] A. G. Hauptmann, J. Gao, R. Yan, Y. Qi, J. Yang, and H. D. Wactlar, "Automated analysis of nursing home observations," *IEEE Pervasive Comput.*, vol. 3, no. 2, pp. 15–21, Apr.–Jun. 2004.
- [21] S. J. Ray and J. Teizer, "Real-time construction worker posture analysis for ergonomics training," *Adv. Eng. Informat.*, vol. 26, no. 2, pp. 439–455, 2012.
- [22] M. C. Schall, N. B. Fethke, H. Chen, and F. Gerr, "A comparison of instrumentation methods to estimate thoracolumbar motion in field-based occupational studies," *Appl. Ergonom.*, vol. 48, pp. 224–231, 2015.
- [23] U. C. Gatti, S. Schneider, and G. C. Migliaccio, "Physiological condition monitoring of construction workers," *Autom. Construction*, vol. 44, pp. 227–233, 2014.
- [24] T. Cheng, G. C. Migliaccio, J. Teizer, and U. C. Gatti, "Data fusion of real-time location sensing and physiological status monitoring for ergonomics analysis of construction workers," *J. Comput. Civil Eng.*, vol. 27, no. 3, pp. 320–335, Oct. 2012.
- [25] J. A. Diego-Mas and J. Alcaide-Marzal, "Using kinect sensor in observational methods for assessing postures at work," *Appl. Ergonom.*, vol. 45, no. 4, pp. 976–985, 2014.
- [26] Z. Zhang, Z. Wu, J. Chen, and J.-K. Wu, "Ubiquitous human body motion capture using micro-sensors," in *Proc. IEEE Int. Conf. Pervasive Comput. Commun.*, 2009, pp. 1–5.
- [27] Z. Zhang, W. C. Wong, and J. Wu, "Wearable sensors for 3d upper limb motion modeling and ubiquitous estimation," *J. Control Theory Appl.*, vol. 9, no. 1, pp. 10–17, 2011.
- [28] B.-H. Yang, S. Rhee, and H. H. Asada, "A twenty-four hour tele-nursing system using a ring sensor," in *Proc. IEEE Int. Conf. Robot. Autom.*, 1998, vol. 1, pp. 387–392.
- [29] F. Naya, R. Ohmura, F. Takayanagi, H. Noma, and K. Kogure, "Workers' routine activity recognition using body movements and location information," in *Proc. 10th IEEE Int. Symp. Wearable Comput.*, 2006, pp. 105–108.
- [30] N. Alshurafa, W. Xu, J. J. Liu, M.-C. Huang, B. J. Mortazavi, and M. Sarrafzadeh, "Designing a robust activity recognition framework for health and exergaming using wearable sensors," *IEEE J. Biomed. Health Inf.*, vol. 18, no. 5, pp. 1636–1646, Sep. 2014.
- [31] S. Kim and M. A. Nussbaum, "An evaluation of classification algorithms for manual material handling tasks based on data obtained using wearable technologies," *Ergonomics*, vol. 57, no. 7, pp. 1040–1051, 2014.
- [32] B. Altakouri, G. Kortuem, A. Grünerbl, K. Kunze, and P. Lukowicz, "The benefit of activity recognition for mobile phone based nursing documentation: A wizard-of-oz study," in *Proc. IEEE Int. Symp. Wearable Comput.*, 2010, pp. 1–4.
- [33] K. Momen and G. R. Fernie, "Nursing activity recognition using an inexpensive game controller: An application to infection control," *Technol. Health Care*, vol. 18, no. 6, pp. 393–408, 2010.
- [34] K. Momen and R. Fernie, "Automatic detection of the onset of nursing activities using accelerometers and adaptive segmentation," *Technol. Health Care: Official J. Eur. Soc. Eng. Med.*, vol. 19, no. 5, pp. 319–329, 2010.
- [35] S. Freitag, R. Ellegast, M. Dulon, and A. Nienhaus, "Quantitative measurement of stressful trunk postures in nursing professions," *Ann. Occupational Hygiene*, vol. 51, no. 4, pp. 385–395, 2007.
- [36] B. Yao and L. Fei-Fei, "Recognizing human-object interactions in still images by modeling the mutual context of objects and human poses," *IEEE Trans. Pattern Anal. Mach. Intell.*, vol. 34, no. 9, pp. 1691–1703, Sep. 2012.
- [37] A. Gupta, A. Kembhavi, and L. S. Davis, "Observing human-object interactions: Using spatial and functional compatibility for recognition," *IEEE Trans. Pattern Anal. Mach. Intell.*, vol. 31, no. 10, pp. 1775–1789, Oct. 2009.
- [38] D. Rebolj, N. Č. Babič, A. Magdič, P. Podbreznik, and M. Pšunder, "Automated construction activity monitoring system," *Adv. Eng. Inf.*, vol. 22, no. 4, pp. 493–503, 2008.
- [39] T. Cheng and J. Teizer, "Real-time resource location data collection and visualization technology for construction safety and activity monitoring applications," *Autom. Construction*, vol. 34, pp. 3–15, 2013.
- [40] S. Malassiotis and M. Srinivas, "Motion estimation based on spatiotemporal warping for very low bit-rate coding," *IEEE Trans. Commun.*, vol. 45, no. 10, pp. 1172–1175, Oct. 1997.
- [41] A. Rav-Acha, Y. Pritch, D. Lischinski, and S. Peleg, "Evolving time fronts: Spatio-temporal video warping," in *Proc. 32nd Int. Conf. Comput. Graph. Interactive Tech.*, 2005, pp. 1–8.
- [42] F. Zhou and F. Torre, "Canonical time warping for alignment of human behavior," in *Proc. Adv. Neural Inf. Process. Syst.*, 2009, pp. 2286–2294.
- [43] Microsoft. Kinect. last accessed April 5 2016. [Online]. Available: <http://www.xbox.com/en-US/xbox-one/accessories/kinect-for-xbox-one>
- [44] NORA Healthcare and Social Assistance Sector. (2013, Feb.). National Occupational Research Agenda (NORA) National Healthcare and Social Assistance Agenda. last accessed April 5 2016. [Online]. Available: <http://www.cdc.gov/niosh/nora/comment/agendas/hlthcaresocassist/>
- [45] F. Lin, A. Wang, C. Song, and W. Xu, "A comparative study of smart insole on real-world step count," in *Proc. IEEE Signal Process. Med. Biol. Symp.*, Philadelphia, PA, USA, Dec. 2015, pp. 1–6.
- [46] W. Xu, M.-C. Huang, N. Amini, J. Liu, L. He, and M. Sarrafzadeh, "Smart insole: A wearable system for gait analysis," in *Proc. Int. Conf. Pervasive Technol. Related Assistive Environ.*, Crete Island, Greece, Jun. 2012, pp. 69–72.
- [47] Y. Wu, W. Xu, J. J. Liu, M.-C. Huang, S. Luan, and Y. Lee, "An energy-efficient adaptive sensing framework for gait monitoring using smart insole," *IEEE Sensors J.*, vol. 15, no. 4, pp. 2335–2343, Apr. 2015.
- [48] W. Xu, Z. Li, M.-C. Huang, N. Amini, and M. Sarrafzadeh, "Ecushion: An extensible device for sitting posture monitoring," in *Proc. IEEE Int. Conf. Body Sensor Netw.*, May 2011, pp. 194–199.
- [49] Bosch Sensortec. BMX055. last accessed April 5 2016. [Online]. Available: http://www.bosch-sensortec.com/bst/products/all_products/bmx055
- [50] Texas Instruments. CC2541 SimpleLink Bluetooth Smart and Proprietary Wireless MCU. last accessed April 5 2016. [Online]. Available: <http://www.ti.com/product/cc2541>
- [51] Y. Rubner, C. Tomasi, and L. J. Guibas, "The earth mover's distance as a metric for image retrieval," *Int. J. Comput. Vis.*, vol. 40, no. 2, pp. 99–121, 2000.
- [52] T. M. Rath and R. Manmatha, "Word image matching using dynamic time warping," in *Proc. IEEE Comput. Vis. Pattern Recog., Conf.*, 2003, vol. 2, pp. II-521–II-527.
- [53] A. Nelson and A. Baptiste, "Evidence-based practices for safe patient handling and movement," *Online J. Issues Nursing*, vol. 9, no. 3, pp. 55–69, 2004.
- [54] C. A. Ratanamahatana and E. Keogh, "Everything you know about dynamic time warping is wrong," in *Proc. 3rd Workshop Mining Temporal Sequential Data*, 2004, pp. 1–11.
- [55] H. Sakoe, S. Chiba, A. Waibel, and K. Lee, "Dynamic programming algorithm optimization for spoken word recognition," *Readings Speech Recog.*, vol. 159, pp. 43–49, 1990.
- [56] N. Krause, R. Rugulies, D. R. Ragland, and S. L. Syme, "Physical workload, ergonomic problems, and incidence of low back injury: A 7.5-year prospective study of san francisco transit operators," *Amer. J. Ind. Med.*, vol. 46, no. 6, pp. 570–585, 2004.
- [57] H. S. Jung and H.-S. Jung, "Establishment of overall workload assessment technique for various tasks and workplaces," *Int. J. Ind. Ergonom.*, vol. 28, no. 6, pp. 341–353, 2001.

- [58] K. H. Brodersen, C. S. Ong, K. E. Stephan, and J. M. Buhmann, "The balanced accuracy and its posterior distribution," in *Proc. 20th Int. Conf. Pattern Recog.*, 2010, pp. 3121–3124.
- [59] O. Pele and M. Werman, "A linear time histogram metric for improved sift matching," in *Proc. Eur. Conf. Comput. Vis.*, 2008, pp. 495–508.
- [60] H. Sakoe and S. Chiba, "Dynamic programming algorithm optimization for spoken word recognition," *IEEE Trans. Acoust., Speech Signal Process.*, vol. 26, no. 1, pp. 43–49, Feb. 1978.
- [61] E. Keogh and C. A. Ratanamahatana, "Exact indexing of dynamic time warping," *Knowl. Inf. Syst.*, vol. 7, no. 3, pp. 358–386, 2005.



Feng Lin (S'11–M'15) received the B.S. degree from Zhejiang University, Hangzhou, China, in 2006, the M.S. degree from Shanghai University, Shanghai, China, in 2009, and the Ph.D. degree from the Department of Electrical and Computer Engineering, Tennessee Tech University, Cookeville, TN, USA, in 2015.

He worked for Alcatel-Lucent from 2009 to 2010. He is currently a Research Scientist at the Department of Computer Science and Engineering, the State University of New York at

Buffalo, Buffalo, NY, USA. His research interests include signal processing, pattern recognition, embedded sensing, human–computer interface, wireless communications, and their applications in wireless health and biometrics.



Aosen Wang (S'15) received the B.S. degree in electrical engineering from the University of Science and Technology of China, Hefei, China, in 2011. He is a third-year Ph.D. student of computer science and engineering at University at Buffalo, State University of New York, Buffalo, NY, USA.

He joined Vimicro as an Algorithm and Software Engineer. His research interests include low-power computer architecture and energy-efficient machine learning.



Lora Cavuoto received the M.S. and Ph.D. degrees in industrial and systems engineering from Virginia Tech, Blacksburg, VA, USA, in 2009 and 2012, respectively. She received the M.S. degree in occupational ergonomics and safety from the University of Miami, Coral Gables, FL, USA, in 2008.

She is currently an Assistant Professor in the Department of Industrial and Systems Engineering, University at Buffalo, Buffalo, NY, USA. She is the Director of the Ergonomics and Biomechanics Laboratory, University at Buffalo. Her current research interests include quantifying physical exposures and physiological responses in the workplace to identify indicators of fatigue development. Her research work also aims to understand and model the effects of health conditions, particularly obesity and aging, on physical capacity, specifically strength, fatigue, and motor performance. She is an Associate Editor for *Human Factors and Ergonomics in Manufacturing & Service Industries* and serves on the Editorial Board for *Applied Ergonomics*.



Wenyao Xu (M'13) received the Ph.D. degree from the Department of Electrical Engineering, University of California, Los Angeles, CA, USA, in 2013.

He is currently an Assistant Professor with the Department of Computer Science and Engineering, the State University of New York at Buffalo, New York, NY, USA. His current research interests include embedded systems, computer architecture, wireless health, internet of things, and their applications in biomedicine, health-care, and security. He owned five licensed U.S. and international patents, and has authored more than 80 peer-reviewed journal and conference papers.

Dr. Xu received the Best Paper Award of the IEEE Conference on Implantable and Wearable Body Sensor Networks in 2013 and the Best Demonstration Award of ACM Wireless Health Conference in 2011.